Fottea, Olomouc, 22(2): 238–255, 2022
DOI: 10.5507/fot.2021.024

A new freshwater species *Conticribra sinica* (Thalassiosirales, Bacillariophyta) from the lower reaches of the Yangtze River, China

Pan Yu[1, 2], Lin Yang[1], Qingmin You[1], Yonghong Bi[2] & Quanxi Wang[1]*

[1]*College of Life Sciences, Shanghai Normal University, Shanghai 200234, P. R. China; *Corresponding author e–mail: wangqx@shnu.edu.cn*
[2]*Institute of Hydrobiology, Chinese Academy of Sciences, Wuhan, 430072, P. R. China*

Abstract: A new freshwater diatom species *Conticribra sinica* sp. nov. Yu, You et Wang from three lakes in the lower reaches of the Yangtze River, China, is described here using a combination of morphological and molecular data from ribosomal DNA genes. The primary distinguishing characteristic of *C. sinica* was the presence of a non–plicate or slightly–plicate valve face and a single ring marginal fultoportulae that was located at the junction between the valve face and the mantle. There were 4–11 valve face fultoportulae that were located at the subcenter of the valve face. In addition, a single rimoportula replaced a marginal fultoportulae. Areolae loculate were open to the outside by irregularly circular foramina or slit foramina that are radially arranged. Internally, cribra were continuously arranged long a radial arrangement of areolae. Characteristics of the new species with other similar species of *Conticribra*. Phylogenetic analysis of the nuclear small subunit (SSU) rDNA sequences and nuclear large subunit (LSU) rDNA gene sequences revealed that *C. sinica* in a single clade at a considerable sequence distance from the other *Conticribra* species.

Key words: diatom, new species, taxonomy, Lancheng Lake, morphology, phylogeny

Introduction

The genus *Conticribra* was established by Stachura–Suchoples & Williams (2009) with *C. tricircularis* Stachura–Suchoples et Williams (Stachura–Suchoples & Williams 2009) as the type species. The genus was originally described from a freshwater Pliocene deposit from Trout Creek, Oregon, USA.. The primary characteristics of this genus include: 1) non–plicated valve faces, 2) a single rimoportula located on the valve mantle that replaces a marginal fultoportulae, and 3) loculate areolae with (semi–)continuous cribra (Stachura–Suchoples & Williams 2009; Park & Lee 2014; Stachura–Suchoples & Kulikovskiy 2014). Only five species have been described within this genus, including two fossil species: *C. tricircularis* and *C. nevadica* (Khursevich et Van Landingham) Stachura–Suchoples et Williams (Stachura–Suchoples & Williams 2009), and three extant species: *C. guillardii* (Hasle) Stachura–Suchoples et Williams (Stachura–Suchoples & Williams 2009), *C. weissflogii* (Grunow) Stachura–Suchoples et Williams (Stachura–Suchoples & Williams 2009), and *C. weissflogiopsis* Park et Lee (Park & Lee 2014).

The two fossil *Conticribra* species, *C. tricircularis* and *C. nevadica* were later transferred to the genus *Spicaticribra* (Johansen et al. 2008) based on the absence of valve face fultoportulae and loculate areolae with (semi–)continuous cribra (Khursevich & Kociolek 2012). The two fossil species are now names of *Spicaticribra tricircularis* (Stachura–Suchoples et Williams) Kociolek et Khursevich (Khursevich & Kociolek 2012) and *S. nevadica* (Stachura–Suchoples et Williams) Kociolek et Khursevich (Khursevich & Kociolek 2012). The presence of valve face fultoportulae is a characteristic that distinguishes living and fossil *Conticribra* species. *C. guillardii* have 0–4 valve face fultoportulae (Hasle 1978), *C. weissflogii* exhibits many valve face fultoportulae on the subcentral area (Fryxell & Hasle 1977), and *C. weissflogiopsis* exhibits 2–12 valve face fultoportulae on the subcentral area (Park & Lee 2014).

Only one species *C. weissflogii* has been reported in China and is distributed within the Shanxi provinces, Guangxi provinces, and Gansu provinces (Qi 1995). In the present study, we describe the new freshwater *Conticribra* species, *C. sinica* from the Liancheng Lake, Poyang Lake and Cao lake in the lower reaches of the Yangtze River, China. Valve morphology is documented with light (LM) and scanning electron microscopy (SEM), followed by comparison to other similar species

within the genus. In addition, molecular phylogenetic comparisons were conducted using ribosomal SSU and LSU rDNA, revealing further differentiation from existing Conticribra species.

Materials and Methods

Sample collection, isolation, and cultures. Diatom samples were collected from three lakes in the lower reaches of the Yangtze River. Samples were collected in August 2018 and 2019 from Liancheng Lake (30°44"N, 116°12'E) is located in Anqing City, Anhui provinces, collected in August, 2018 and 2019. Poyang Lake (28º22'–29°45'N, 115°47'–116°45'E) is located at the junction of the middle and lower reaches of Yangtze River, it is the largest freshwater lake in China, collected in August, 2017. Cao Lake (31°29'N, 120°34'E) is located in Suzhou City, Jiangsu Province, collected in August, 2018. In the field, several water chemistry characteristics were recorded, including: pH, temperature, dissolved oxygen, total dissolved solids (TDS), and conductivity (EC). These were all measured using a YSIPro Plus multiparameter meter (YSI, Ohio, USA). Diatom samples were collected from natural substrates, including stones, Fishing net, and navigation buoys, by brushing with clean toothbrushes. Samples were placed in sample bottles and preserved with formalin at a 4% final concentration.

Live sample was collected one location in Liancheng Lake, and single diatom cells derived from clone cultures of subsamples were isolated using a Pasteur pipette and the capillary method under a Nikon Ts2 inverted microscope (NIKON, Tokyo, Japan). Cells were isolated and cultured in 24 well cell plates, with each well containing 2 ml of CSI medium. Non–axenic unialgal cultures were maintained in CSI medium at 24 °C in a growth chamber under a 12:12 h light/dark photoperiod. Nucleotide sequences of SSU rDNA and LSU rDNA nucleotide sequences for strains LCH18 and LCH 2D3 were deposited in GenBank (NCBI), with accession numbers MZ226431, MZ226430, MZ226433, and MZ226432, respectively.

LM and SEM analysis. In the laboratory, diatom samples were cleaned with concentrated nitric acid using a Microwave Accelerated Reaction System (Model MARS, CEM Corporation, Charlotte, USA) (Parr et al. 2004), with a pre–programmed digestion scheme (temperature, 180 °C) (Yu et al. 2019). Next, samples were alternately centrifuged for 8 min at 3000 rpm (TDZ5–WS, Luyi Corporation, Shanghai, China) and washed five times using distilled water. The resulting diatom samples were preserved with 95% ethanol. Permanent diatom slides were made with Naphrax for light microscopy (LM) and cleaned diatom samples were air–dried onto cover slips and mounted onto alloy stubs for observation with the scanning electron microscope (SEM). LM observations were made with a ZEISS AXIO Imager A2 microscope fitted with DIC optics and at 1000× magnification (1.4 numerical aperture). SEM observations were made using a SU8010 instrument (Hitachi High–Technologies Corp., Tokyo, Japan) at 2 kV, and with a working distance of less than 6 mm. Images were compiled with Adobe Photoshop CS6 (Adobe Systems Inc., San Jose, C.A., U.S.A.). Morphological terminology follows Round et al. (1990). All of the diatom samples and permanent slides are deposited at the Biology Department Diatom Herbarium, Shanghai Normal University (SHTU).

Table 1. Sampling sites and their geographical and chemical characteristics.

Sample number	Collection site	Habitat	Longitude and Latitude	WT	pH	EC (μS.cm^{-1})	TN (mg.l^{-1})	TP (mg.l^{-1})	COD (mg.l^{-1})	TDS (mg.l^{-1})
LCH201908–Z2	Liancheng Lake	Stone	30°43'37"N, 117°11'41"E	32.2	9.90	232.6	2.3	0.29	36.8	132.6
LCH201808–Z1	Liancheng Lake	Stone	30°43'30"N, 117°12'15"E	33.7	8.99	281.9	2.3	0.23	37.2	157.3
PYH201708–Z16	Poyang Lake	Navigation buoys	29°17'3"N, 116°0'16"E	30.3	8.67	123.0	0.7	0.06	6.4	82
PYH201708–Z37	Poyang Lake	Fishing nets	28°46'13"N, 116°22'34"E	32.2	7.11	107.0	2.2	0.1	4.5	53
PYH201708–P56	Poyang Lake	Planktonic	28°39'56"N, 116°20'53"E	36.3	6.23	113.0	1.5	0.1	13.4	56
CH201808–Z1	Cao Lake	Stone	31°28'44"N, 120°34'37"E	33.8	8.86	719.0	1.1	0.22	17.9	403

Fottea, Olomouc, 22(2): 238–255, 2022
DOI: 10.5507/fot.2021.024

Table 2. Parameters of the nucleotide substitution model estimates using Modeltest v3.7.

Molecular marker	Model selected	Base frequency	Rate matrix
LSU rDNA + SSU rDNA	TrN+I+G		R(a)[A–C] = 1.0000
	–lnL = 8657.2246	freqA = 0.2574	R(b)[A–G] =3.0123
	K = 7	freqC = 0.1962	R(c)[A–T] = 1.0000
	(I) = 0.5406	freqG = 0.2642	R(d)[C–G] = 1.0000
	(G) = 0.4614	freqT = 0.2822	R(e)[C–T] = 5.2484
			R(f)[G–T] = 1.0000

Extraction of DNA and gene amplification. The total DNA of monoclonal culture strains was extracted using the InstaGeneTM Matrix following the manufacturer's protocols. Fragments of SSU rDNA (~1,750 nt) and LSU rDNA (~600 nt) genes were amplified by PCR using the primers 11F and 1174R for SSU rDNA fragments, in addition to D1R and D2C for LSU rDNA fragments (Alverson et al. 2007).

Amplifications of SSU rDNA fragments were conducted using a premade ScreenMix (Evrogen, Moscow, Russia) for PCR assays. Amplification conditions for the SSU rDNA fragments included an initial denaturation for 3.5 min at 94 °C, followed by 35 cycles of denaturation at 94 °C for 50 s, annealing at 58 °C for 50 s, and extension at 72 °C for 60 s, all followed by a final extension at 72 °C for 10 min. The amplification conditions for LSU rDNA fragments included an initial denaturation for 3.5 min at 94 °C, followed by 35 cycles of denaturation for 35 cycles at 94 °C for 50 s, annealing at 51 °C for 50 s, and extension at 72 °C for 60 s, all followed by a final extension at 72 °C for 10 min. Each PCR mixture (50 µl) contained 17 µl of ddH_2O, 25 µl of 2×EasyTaq PCR SuperMix (TransGen Biotech, Beijing, China), 2 µl of each primer (10 mM) (BGI, Shanghai, China), and 4 µl of DNA template.

PCR products were purified using a SanPrep column DNA gel purification kit (Sangon, China), and then sent to the BGI Tech Corporation (Beijing, China) for sequencing on an ABI 3730XL sequencer. Sequences were compared to the National Center for Biotechnology Information (NCBI) using BLAST searches to identify closely related sequences.

Phylogenetic tree construction. rDNA sequences from this study and references from the NCBI Genbank database were collected representing 51 centric diatoms from different morphological groups and included in the alignments (Table S1). *Bellerochea malleus*, was used as the outgroup taxon.
Sequences were aligned with ClustalW in the BioEdit sequence analysis software (Thompson et al. 1997; Hall 1999). Untrimmed bases from both ends were deleted to produce identical length alignments. The jModelTest v3.7 Software program was used to identify the optimal nucleotide substitution model, resulting in the selection of the GTR model of nucleotide substitutions with gamma (G) distribution rates and equal proportions across invariable sites (I) as the most appropriate evolutionary model all of the rDNA alignments (Posada 2006) (Table 2). Concatenated SSU rDNA + LSU rDNA alignments for 52 taxa were produced and phylogenies were constructed based on the above substitution model using Bayesian Inference (BI) and Maximum Likelihood (ML) analyses. The PHYML software program was used to generate ML trees and bootstrap analysis was conducted using 1,000 replicates to estimate node support (Felsenstein 1981; Guindon & Gascuel 2003). Bayesian analyses were conducted using MrBayes v3.1.2. The Markov Chain Monte Carlo (MCMC) algorithm was used to estimate the posterior probabilities of phylogenetic trees by simultaneously running three hot Markov chains in addition to one cold Markov chain. The Markov chains started from a random tree and ran for 2,000,000 generations, with sampling every 1,000 generations, comprising a total of 2,000 samples for each run. FigTree v1.4.2 and Adobe Illustrator CS6 were used to visualize the resulting phylogenetic trees. Figure 119 shows the Maximum Likelihood phylogenetic tree topology derived from the analysis of the concatenated SSU rDNA + LSU rDNA sequence datasets.

Results

Class Bacillariophyceae Haeckel emend. Medlin et Kaczmarska (Medlin & Kaczmarska 2004)
Subclass Thalassiosirophycidae Round et Crawford in Round et al. (Round et al. 1990)
Order Thalassiosirales Glezer et Makarova in Round et al. (Round et al. 1990)
Family Thalassiosiraceae Lebour in Round et al. (Round et al. 1990)

***Conticribra sinica* Yu, You et Wang sp. nov. (Figs 1–118)**
Description: LM observations (Figs 1–71), Frustule solitary, rectangular in girdle view, numerous slightly lobed chloroplasts present on valve face and girdle in each cell (Figs 1–4). Valves circular with valve face non–plicate or slightly–plicate, slightly convex girdle, valve diameter 13–22 µm (n=100) (Figs 4–71). Perralvar axis shorter than valve diameter, 6.5–15 µm. Valve face and marginal fultoportulae distinctly visible in light microscope, a single ring marginal fultoportulae located on junction between valve face and mantle. 4–11 valve face fultoportulae arranged in a irregular circular ring located on subcenter of valve face, rimoportula identical to marginal fultoportulae.

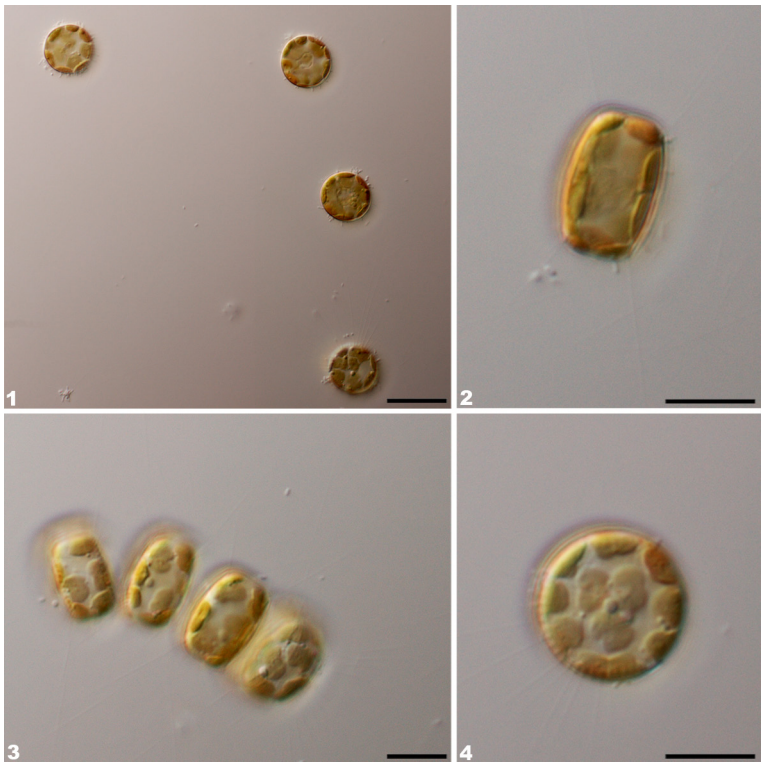

Figs 1–4. Live *Conticribra sinica* sp. nov. cells with chloroplast structure and frustule shape under laboratory culture conditions: (1) single cells; (2–3) girdle view with slightly lobed chloroplasts; (4) valve view with numbers slightly lobe chloroplasts. Scale bars 20 μm (1), 10 μm (2–4).

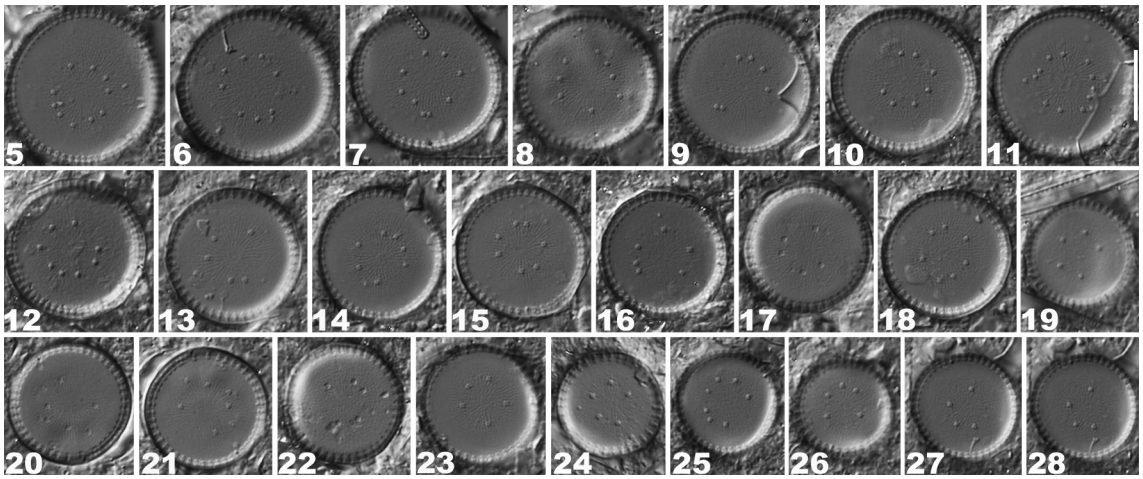

Figs 5–28. LM valve views of *Conticribra sinica* sp. nov. with under field-collected condition. The holotype is illustrated in figure 10. Scale bar 10 μm.

SEM observations (Figs 82–118), externally, areolae loculate, open to outside by irregularly circular foramina or slit foramina, radially arranged, thus, it was difficult to measure the dense areolae (Figs 72–74, 83–85, 89–91, 96–97). Areolae composed of complex frameworks, them into at least two layers for simplification (Figs 77, 101–106). A single ring marginal fultoportulae located on junction between valve face and mantle, number of these processes ranges from 11–15/10 μm (Figs 72–74, 83–85, 88, 89–91, 96–100). External tube of the marginal fultoportulae had a long tubular extension and surrounding several thin siliceous wrinkles (Figs 77, 101–104). 4–11 valve face fultoportulae arranged in a irregular circular ring located on subcenter of valve face (Figs 72–74, 83–85, 88, 89–91, 96–97). The valve face fultoportulae was shorter than the marginal fultoportulae and exhibited several thin siliceous wrinkles surrounding the external tube (Fig. 79). In addition, the valve face fultoportulae were surrounded by some bigger areolae (Figs 105–105). A single rimoportula located on junction between valve face and mantle, and replaced a marginal fultoportulae, and externally appears as a long tube of the same size as the marginal fultoportulae processes (Figs 73, 85, 89–90).

Cribra were continuously arranged internally along a radial arrangement of areolae (Figs 75, 86–87, 92–94).

Fottea, Olomouc, 22(2): 238–255, 2022
DOI: 10.5507/fot.2021.024

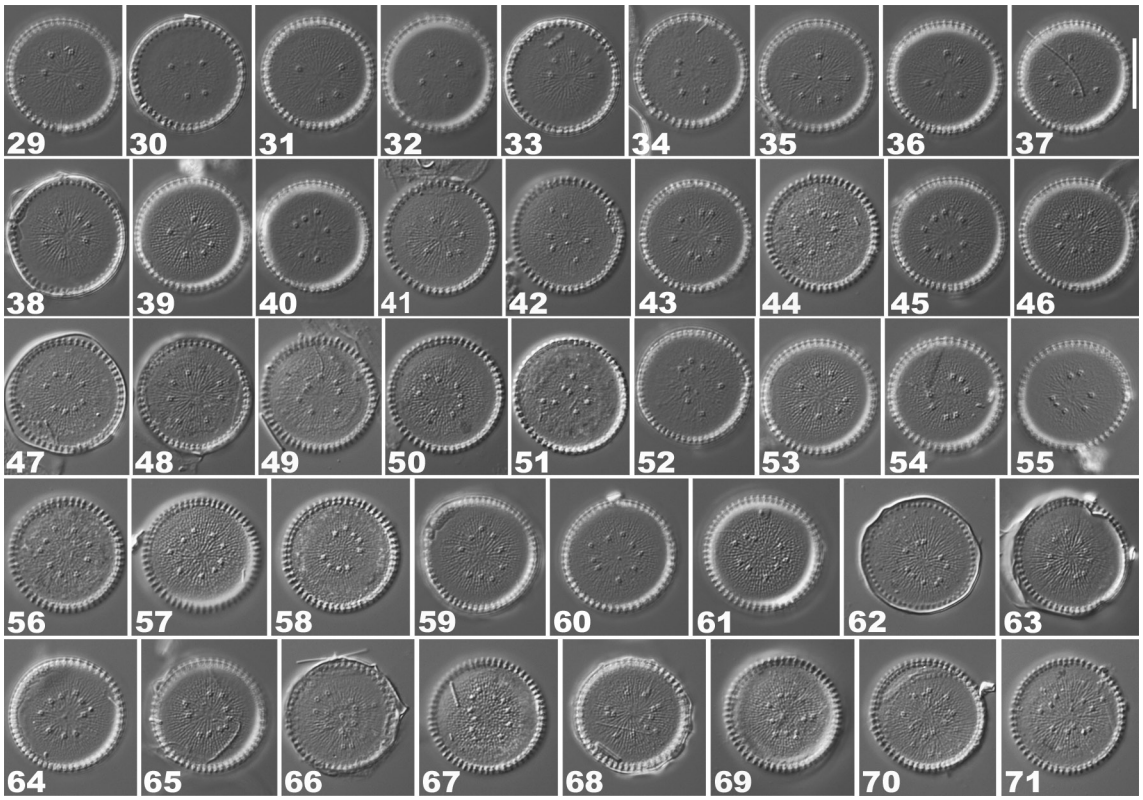

Figs 29–71. LM valve views of *Conticribra sinica* sp. nov. with under laboratory culture condition. Scale bar 10 μm.

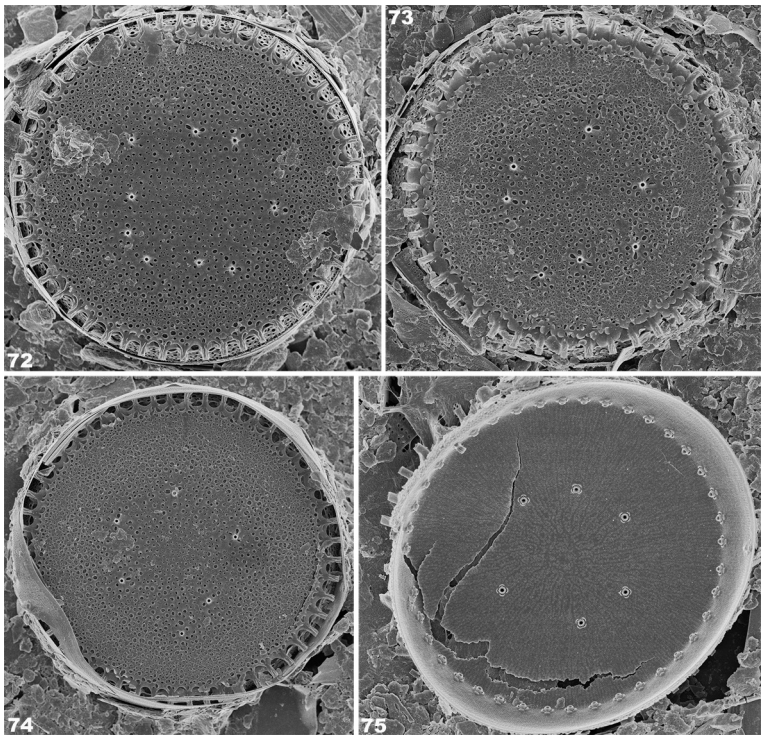

Figs 72–75. *Conticribra sinica* sp. nov. SEM view with under field-collected condition: (72–74) entire external valve view, with a ring of marginal fultoportulae and a irregular ring of valve face fultoportulae (6–9); (75) entire internal valve view, one rimoportula located on the valve mantle and replaced a fultoportula. Scale bars 5 μm (72–74), 2 μm (75).

Marginal fultoportulae surrounded by four satellite pores and each satellite pores covered by a triangular–shaped satellite pore cover, with the cowling structure slightly raised beside the satellite pores (Figs 81, 110–111). Valve face fultoportulae surrounded by 3–4 (typically 4) satellite pores, each with similar pore cover shapes and cowling structures (Figs 80, 107–109). A single rimoportula replaced a marginal fultoportulae, and the rimoportula had a thickened labiate opening, obliquely oriented on a short stalk (Figs 82, 111–112).

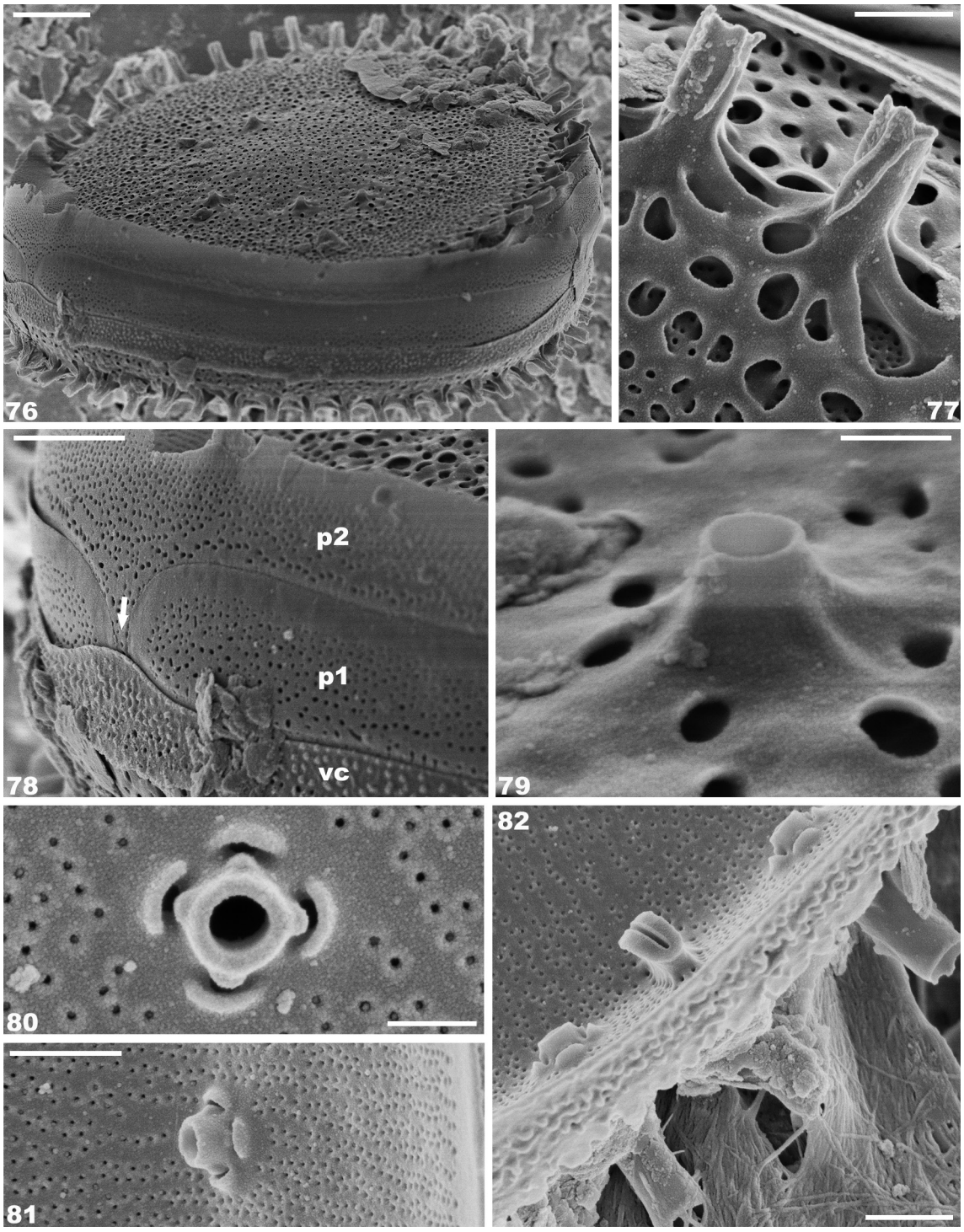

Figs 76–82. *Conticribra sinica* sp. nov. SEM, external views with under field-collected condition: (76) girdle view; (77) external view of marginal fultoportulae, several thin siliceous wrinkles surround the external tube of the fultoportulae; (78) enlarged view of girdle. White arrow indicates the ligula. vc: valvocopula, p: pleura, each number of pleura indicates the band sequences; (79) enlarged view of external view of valve face fultoportulae, tube of the valve face fultoportulae is shorter than the marginal fultoportulae; (80–81) enlarged view of valve face fultoportulae and marginal fultoportulae, each satellite pore was covered by a triangular-shaped satellite pore cover, and the cowling structure is slightly raised beside the satellite pores; (82) internal structure view of the rimoportula. Scale bars 2 μm (75), 1 μm (78, 82), 0.5 μm (77, 81), 0.2 μm (79–80).

Epicingulum consisted of 4 to 12 open bands, each of the band had a fine pore in the advalvar part (Figs 100, 113–118). Valvocopula arranged two rows fine pores and arranged some granules on whole valvocopula (Figs 78, 117, 115). Moreover, adjacent pleura band had fine pores with antiligula in the advalvar part, and pleura part lacked minute granules (Figs 78, 113, 115–118).

Molecular analyses: Pairwise comparisons of rDNA sequences from putatively related taxa demonstrated that *Conticribra sinica* strains exhibited 100% similarity in

Fottea, Olomouc, 22(2): 238–255, 2022
DOI: 10.5507/fot.2021.024

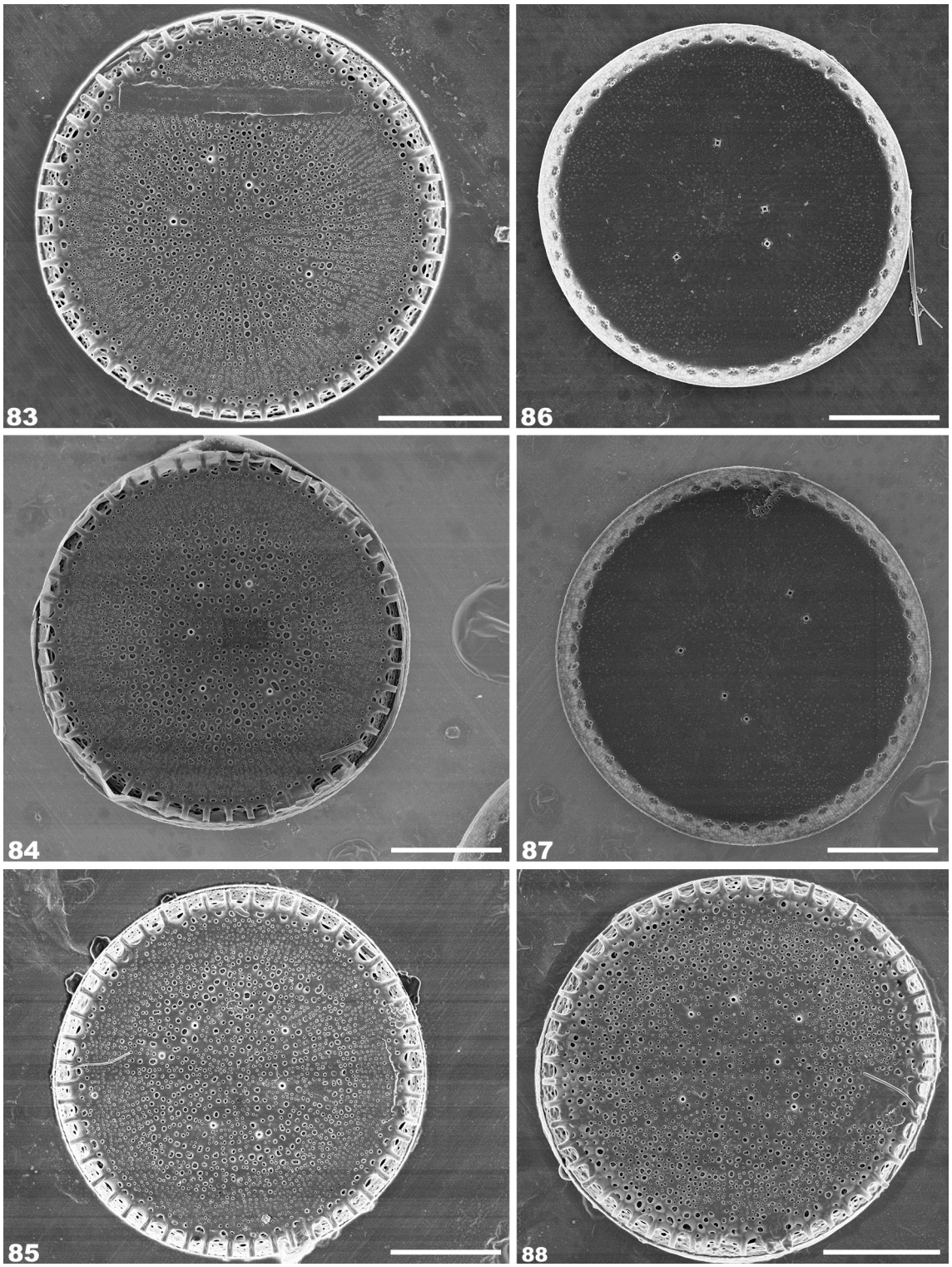

Figs 83–88. *Conticribra sinica* sp. nov. SEM view with under laboratory culture condition: (83–85, 88) entire external valve view, with a ring of marginal fultoportulae and a irregular ring of valve face fultoportulae (4–6); (86–87) entire internal valve view, one rimoportula located on the valve mantle and replaced a fultoportula. Scale bar 5 μm.

rDNA sequences. However, *C. sinica* sequences shared SSU rDNA gene evolutionary distances of 0.03–0.04 with other *Conticribra* diatoms and p–distances of 0.03–0.04 with *Thalassiosira* species. p–distances in SSU rDNA genes between *Thalassiosira* species ranged from 0.00–0.03 (Table 3). The pairwise uncorrected p–distances of partial LSU rDNA genes between the two *C. sinica* strains were 0.00, indicating that they were identical. These strains also exhibited LSU rDNA gene p–distances that ranged from 0.07–0.09 against other *Conticribra* species and from 0.07–0.15 against *Thalassiosira* species. The LSU rDNA gene p–distances between *Thalassiosira* species

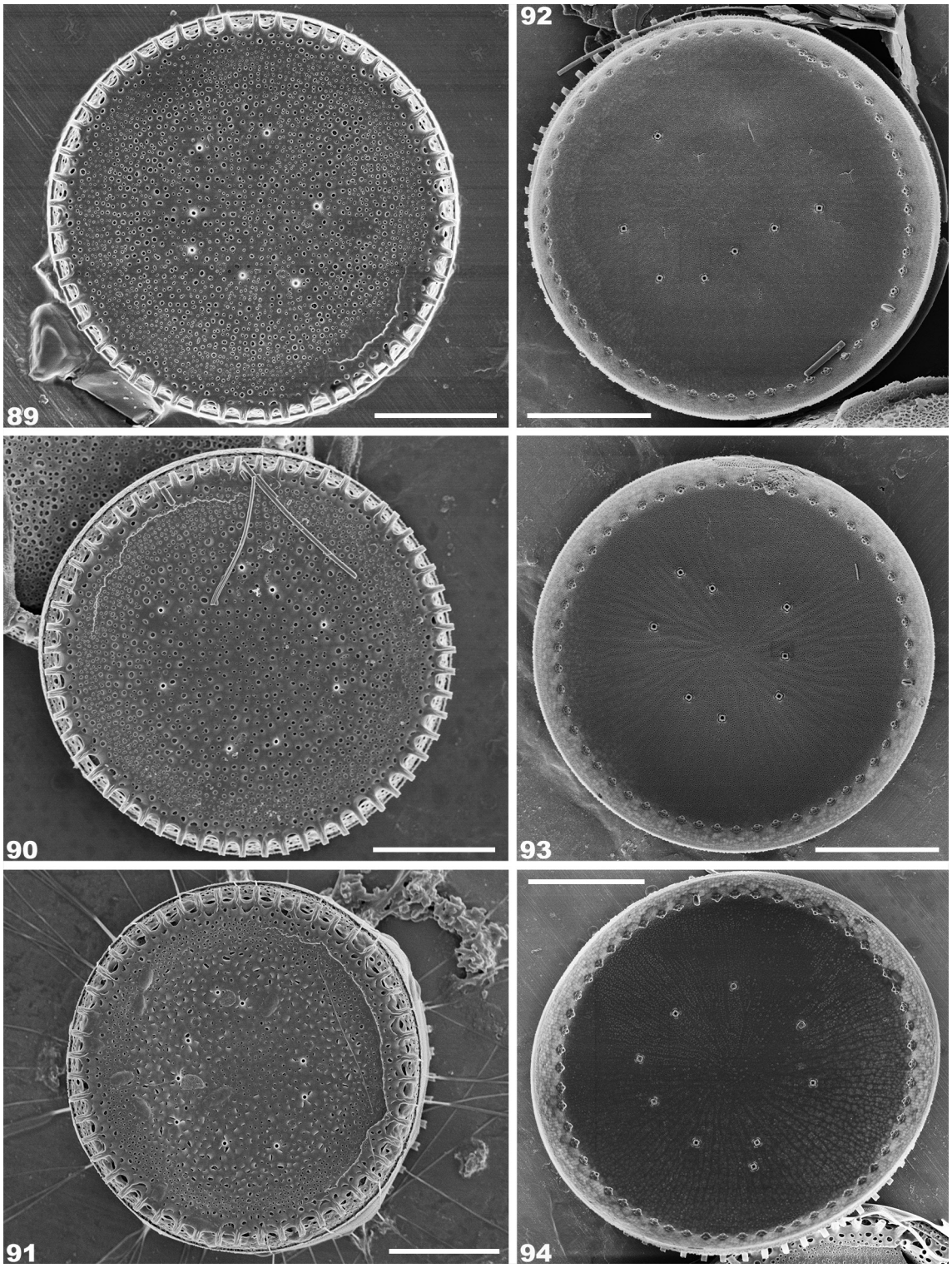

Figs 89–94. *Conticribra sinica* sp. nov. SEM view with under laboratory culture condition: (89–89) entire external valve view, with a ring of marginal fultoportulae and a irregular ring of valve face fultoportulae (7–9); (92–94) entire internal valve view, one rimoportula located on the valve mantle and replaced a fultoportula. Scale bar 5 μm.

also ranged from 0.02–0.14 (Table 4).

The SSU and LSU rDNA gene markers were included in phylogenetic inference analysis using ML and BI methods (Fig. 119). Both analyses resulted in similar phylogenetic topologies. Specifically, *C. sinica* was placed within a large cluster with other *Conticribra* species, although this clade was not well supported by bootstrap scores (BPP/ML<0.5). The two strains of *C. sinica* shared identical alignments, as indicated above. All of the other *Conticribra* species were present within a single clade that had moderate bootstrap support (BPP/ML: 0.96/82.3). In addition, the *Thalassiosira* taxa were

Fottea, Olomouc, 22(2): 238–255, 2022
DOI: 10.5507/fot.2021.024

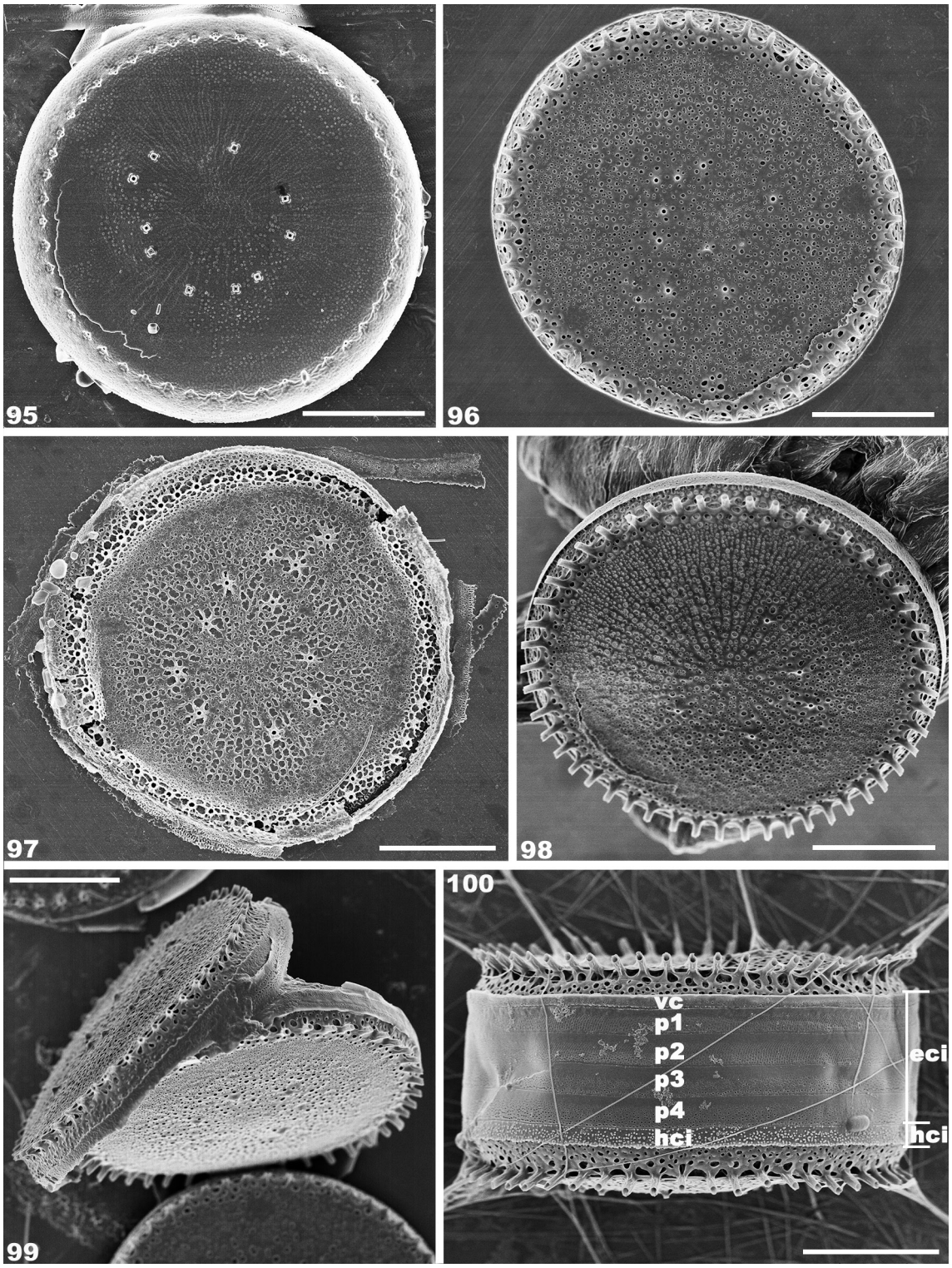

Figs 95–100. *Conticribra sinica* sp. nov. SEM view with under laboratory culture condition: (95) entire internal valve view, one rimoportula located on the valve mantle and replaced a fultoportula; (96–98) entire external valve view, with a ring of marginal fultoportulae and a irregular ring of valve face fultoportulae (10–11); (99–100) girdle view, (100) girdle view showing the opposite side of the fultoportulae (eci: epicingulum, vc: valvocopula, hci: hypocingulum, p: pleura, each number of pleura indicates the band sequences). Scale bar 5 μm.

placed into two clades, while *T. pseudonana* was associated with *Cyclotella* taxa and *T. oceanica* represented a single branch. Among the remaining centric diatoms, they formed a large clade with Stephanodiscaceae taxa that included the genera *Stephanodiscus*, *Cyclostephanos*, *Lindavia*, and *Discostella*.

Holotype (designated here): SHTU! Slide LCH201908–Z2 in Lab of Algae and Environment, College of Life Sciences, Shanghai Normal University, Shanghai, China.

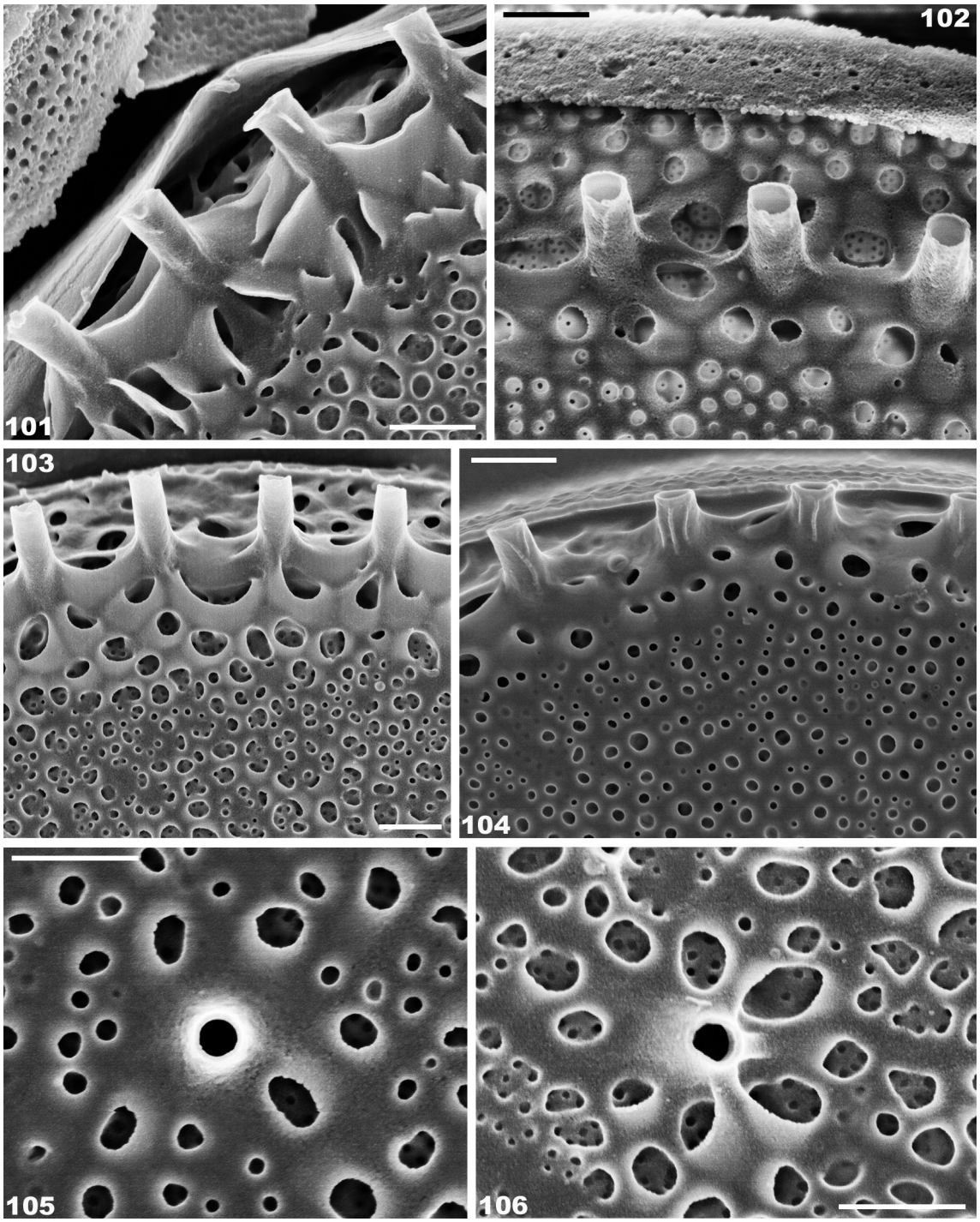

Figs 101–106. *Conticribra sinica* sp. nov. SEM, external valve views with under laboratory culture condition: (101–104) external view of marginal fultoportulae, several thin siliceous wrinkles surround the external tube of the fultoportulae; (105–106) external view of valve face fultoportulae, some bigger areolae surround the external tube of the valve face fultoportulae. Scale bar 0.5 μm.

Holotype illustrated in Fig. 10.

Type locality: China. Liancheng lake, Anhui Province, 30°44'3"N, 117°11'54"E. collected by Quanxi Wang, 23th August 2019.

Habitat: Epiphyton were collected from on stone, fishing nets and navigation buoys. Planktonic were identified in lakes.

Etymology: The species is named refers China where the holotype was collected.

Ecology: Periphytic diatom samples collected in Liancheng Lake (LCH201908–Z2 and LCH201808–Z1), Caohu Lake (CH201808–Z1) and Poyang Lake (PYH201708–Z16 and PYH201708–Z37). Planktonic diatom sample collected in Poyang Lake (PYH201708–P56). For detailed collection information see Table 1.

Distribution: The new species is known from three lakes, include Liancheng Lake, Caohu Lake and Poyang Lake.

Fottea, Olomouc, 22(2): 238–255, 2022
DOI: 10.5507/fot.2021.024

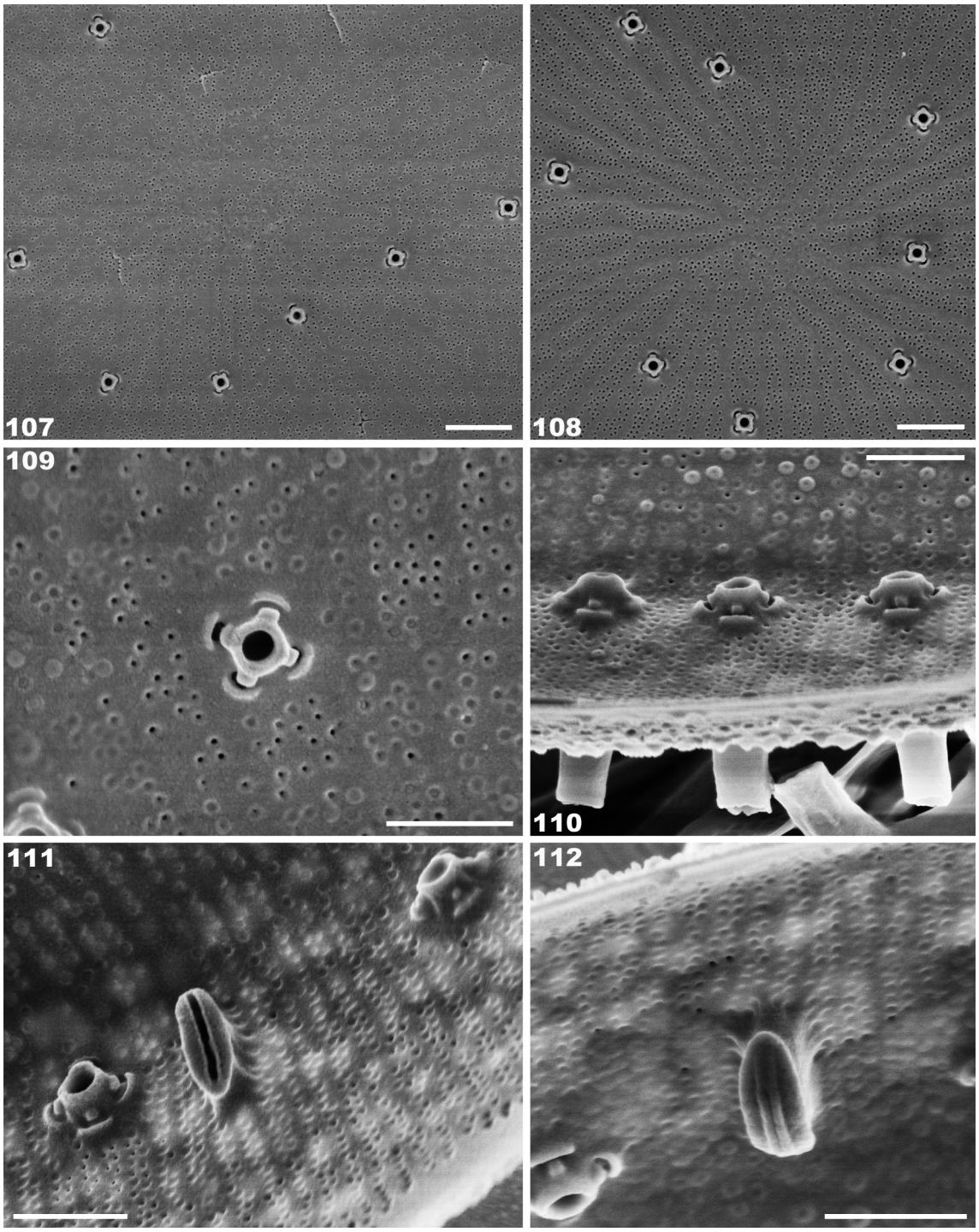

Figs 107–112. *Conticribra sinica* sp. nov. SEM, internal valve views with under laboratory culture condition: (107–109) internal view of valve face fultoportulae, each possessing three or four (usually four) satellite, (109) enlarged view of valve face fultoportulae, each satellite pore is covered by a triangular-shaped satellite pore cover, and the cowling structure is slightly raised beside the satellite pores; (110–111) internal view of marginal fultoportulae, each possessing four satellite, each satellite pore is covered by a triangular-shaped satellite pore cover, and the cowling structure is slightly raised beside the satellite pores; (111–112) internal view of rimoportula. Scale bars 1 μm (107), 0.5 μm (108–112).

Discussion

Conticribra sinica is a new diatom species that possess certain characteristics that support their classification in the genus *Conticribra*, including: flatted valve, loculate areolae with continuous cribra, and the presence of a single rimoportula located at the junction between the valve face and mantle that replaced a marginal fultoportulae (Stachura–Suchoples & Williams 2009).

Based on the outline and structure of their valves,*C. sinica* was similar to other *Conticribra* species including, *C. tricircularis*, *C. nevadica*, *C. guillardii* (Hasle) Stachura–Suchoples et Williams (Stachura–Suchoples

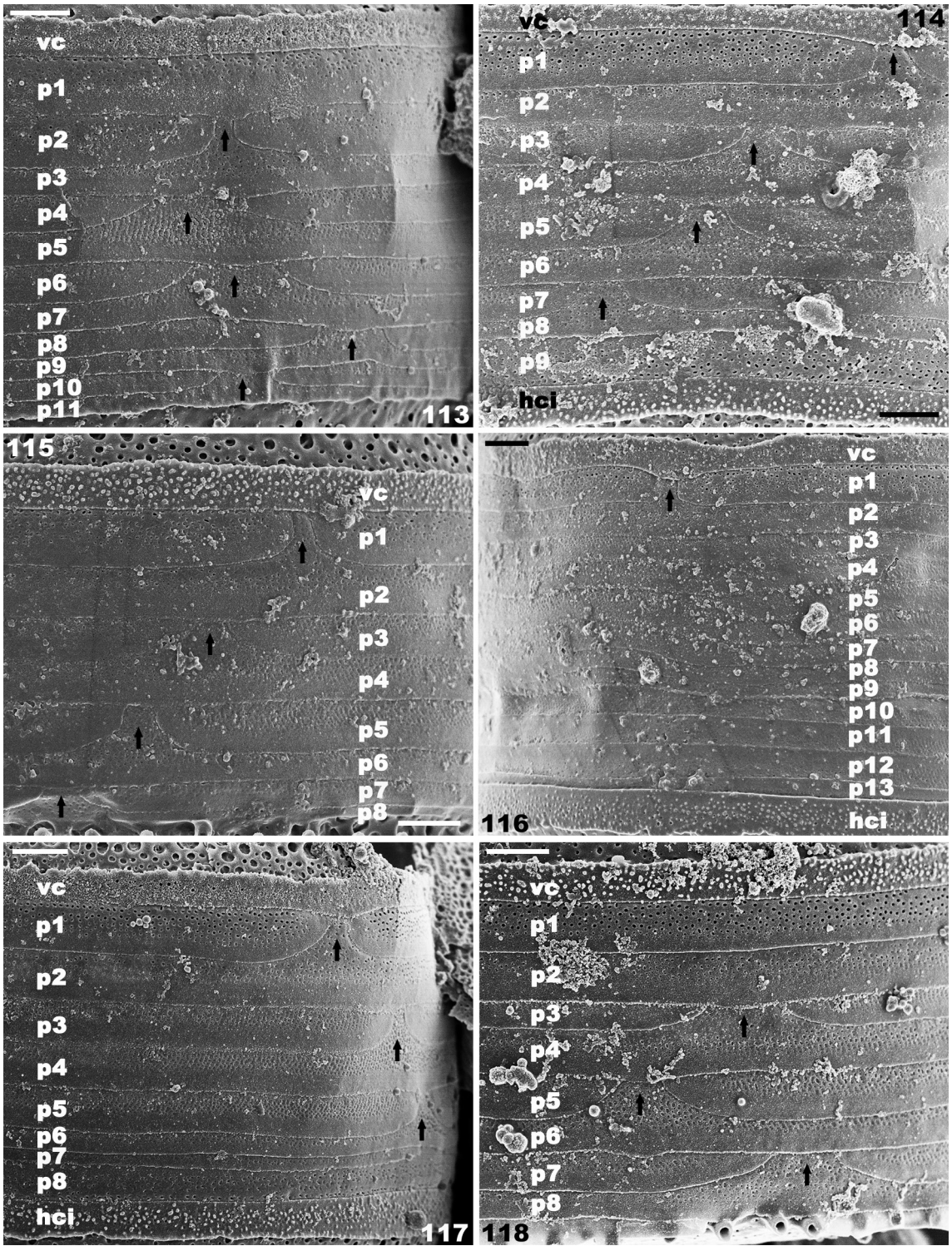

Figs 113–118. *Conticribra sinica* sp. nov. SEM, Enlarged view of girdle with under laboratory culture condition. Black arrow indicates the ligula, vc: valvocopula, hci: hypocingulum, p: pleura, each number of pleura indicates the band sequences. Scale bar 1 μm.

& Williams 2009), *C. weissflogii* (Grunow) Stachura–Suchoples et Williams (Stachura–Suchoples & Williams 2009), and *C. weissflogiopsis* Park et Lee (Park & Lee 2014). The primary characteristics observed in the new species and other related species are summarized in Table 5. The cribra of *C. sinica* are continuous, although those of *C. nevadica* are semi–continuous, and those of *C. tricircularis* are (semi–)continuous. The valve diameter of *C. sinica* (13–21.7 μm) is longer than that of *C. guillardi* (4–14 μm), but shorter than that of *C. tricircularis* (22–29 μm). *C. sinica* only exhibits one ring marginal fultoportulae, but *C. tricircularis* harbors three rings. In addition, the density marginal fultoportulae in *C. sinica* (11–15/10 μm) is higher than for *C. nevadica* (8–10/10

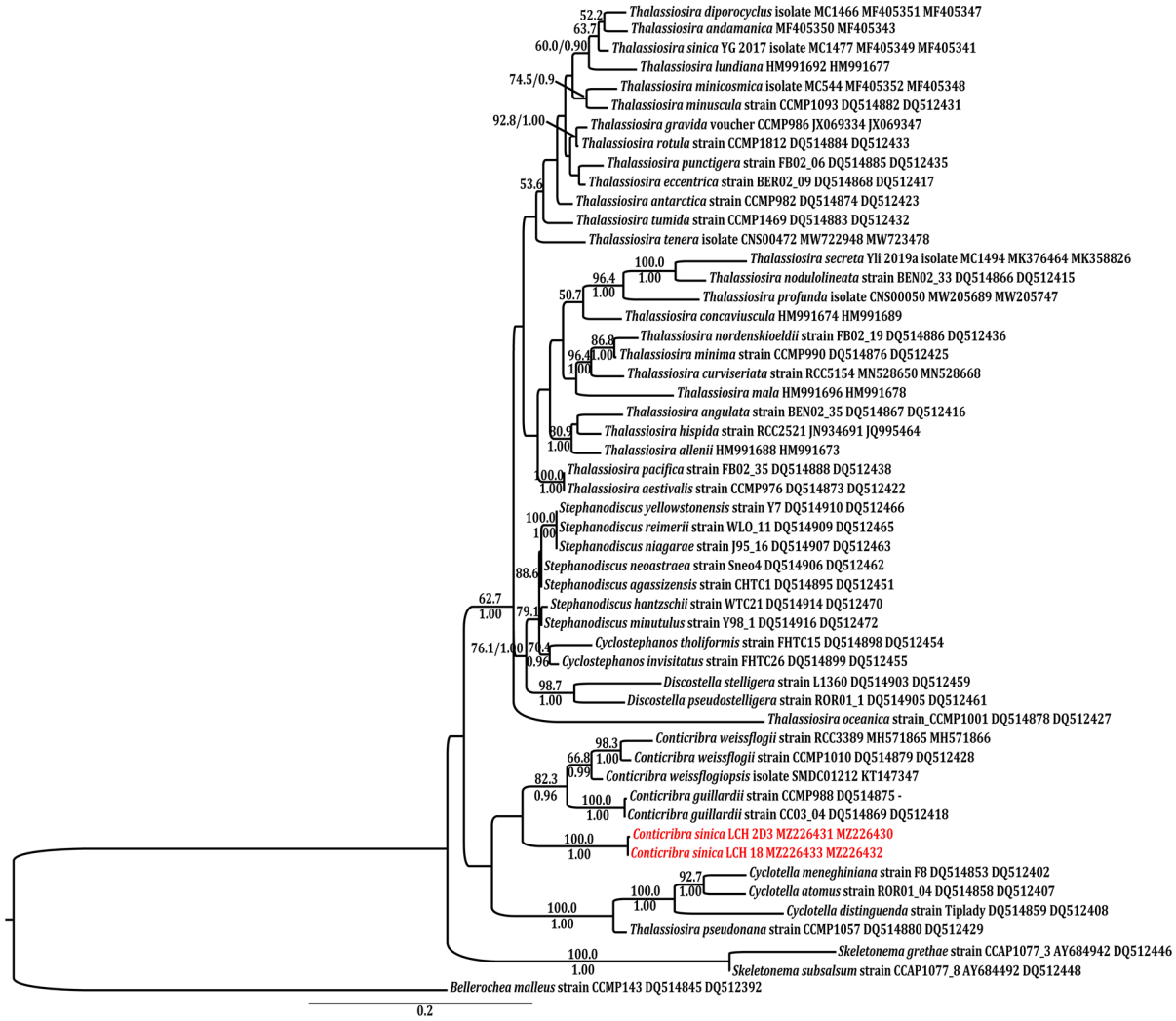

Fig. 119. Maximum likelihood tree of *Conticribra* and *Thalassiosira* species constructed from a concatenated alignment of 52 partial SSU rDNA and LSU rDNA sequences of 1,446 characters. Bootstrap support values obtained from the RAxML analyses are shown above the horizontal lines; values< 50 are not shown. Bayesian posterior probabilities are shown below the horizontal lines; values< 50 are not shown. All sequences have associated strain numbers (if available) and GenBank numbers (Table S1). *Bellerochea malleus* was used as the outgroup. Sequences of our culture strains that were new species in this paper are highlighted in red.

µm), *C. guillardii* (7–8/10 µm), and *C. weissflogiopsis* (10–12/10 µm). Furthermore, the number of valve face fultoportulae in *C. sinica* (4–12) is higher than in *C. guillardii* (0–4), in addition to *C. tricircularis* and *C. nevadica* that both did not exhibit valve face fultoportulae. Moreover, the satellite pores numbers of valve face fultoportulae in *C. sinica* (3–4, but typically 4) differs from those in *C. guillardii* (2–4), *C. weissflogii* (3–5), and *C. weissflogiopsis* (3–4).

Phylogenetic analysis of centric diatom Thalassiosirales Nuclear SSU rDNA sequences and LSU rDNA sequences was previously conducted, indicating that *Thalassiosira* taxa clustered into several large clades (Kaczmarska et al. 2006; Alverson et al. 2007; Li et al. 2018; Li et al. 2020; This study). Thus, the genus *Thalassiosira* comprises a monophyletic group. Phylogenetic analysis in this study based on SSU rDNA and LSU rDNA sequences demonstrated that *Conticribra sinica* was distinct from other *Conticribra* species. Consequently, differences in both morphological measurements and molecular analyses supported the recognition of *Conticribra sinica* as a new species. Relatively small intraspecific genetic variation (< 0.01 p–distance) was observed among the rDNA sequences of *C.sinica*, *C. guillardii* and *C. weissflogii* but larger inter–specific genetic variation was observed when comparing *C. weissflogiopsis* vs. *C. weissflogii* and *C. weissflogiopsis* vs. *C. guillardii* (i.e., 0.01 – 0.06 p–distances). This was especially evident for the two strains of *C. sinica*, which exhibited the largest inter–specific genetic distance with the other *Conticribra* species (i.e., 0.03 – 0.09 p–distances). These sequence comparisons are consistent with those from Park et al. (Park et al. 2014), and the topology of clustering patterns in our phylogenetic analysis.

Species with (semi–)continuous cribra, non–plicate valves, and rimoportula replacing marginal fultoportulae are the primary characteristics of the genus *Conticribra*

Table 3. Pairwise uncorrected p–distances of 20 strains based on the partial SSU rDNA gene.

	1	**2**	**3**	**4**	**5**	**6**	**7**	**8**	**9**	**10**	**11**	**12**	**13**	**14**	**15**	**16**	**17**	**18**	**19**	**20**
1. *Conticribra sinica* strain LCH 2D3	0.00																			
2. *Conticribra sinica* strain LCH18	0.00																			
3. *Conticribra weissflogii* strain CCMP1010	0.03	0.03																		
4. *Conticribra weissflogii* strain RCC3389	0.04	0.04	0.00																	
5. *Conticribra guillardii* strain CC03–04	0.03	0.03	0.02	0.02																
6. *Conticribra guillardii* strain CCMP988	0.03	0.03	0.02	0.02	0.00															
7. *Conticribra weissflogiopsis* isolate SMDC01212	0.03	0.03	0.01	0.01	0.01	0.01														
8. *Thalassiosira minuscula* strain CCMP1093	0.03	0.03	0.04	0.04	0.04	0.03	0.03													
9. *Thalassiosira gravida* voucher CCMP986	0.03	0.03	0.04	0.04	0.04	0.04	0.04	0.01												
10. *Thalassiosira punctigera* strain FB02–06	0.03	0.03	0.04	0.04	0.04	0.04	0.04	0.01	0.01											
11. *Thalassiosira nordenskioeldii* strain FB02–19	0.03	0.03	0.04	0.04	0.04	0.04	0.04	0.02	0.02	0.02										
12. *Thalassiosira profunda* isolate CNS00050	0.04	0.04	0.05	0.05	0.04	0.04	0.04	0.02	0.02	0.03	0.03									
13. *Thalassiosira curviseriata* strain RCC5154	0.03	0.03	0.04	0.04	0.04	0.04	0.04	0.01	0.02	0.02	0.02	0.02								
14. *Thalassiosira nodulolineata* strain BEN02–33	0.04	0.04	0.04	0.05	0.04	0.04	0.04	0.03	0.02	0.03	0.03	0.02	0.03							
15. *Thalassiosira secreta* Yli–2019a isolate MC1494	0.04	0.04	0.03	0.04	0.03	0.03	0.03	0.02	0.02	0.02	0.03	0.02	0.02	0.01						
16. *Thalassiosira minima* strain CCMP990	0.03	0.03	0.04	0.04	0.04	0.04	0.04	0.02	0.02	0.02	0.00	0.03	0.02	0.03	0.02					
17. *Thalassiosira hispida* strain RCC2521	0.03	0.03	0.03	0.04	0.03	0.03	0.03	0.01	0.02	0.02	0.02	0.02	0.02	0.03	0.02	0.02				
18. *Thalassiosira diporocyclus* isolate MC1466	0.03	0.03	0.04	0.04	0.04	0.04	0.03	0.01	0.01	0.01	0.02	0.02	0.02	0.02	0.02	0.02	0.02			
19. *Thalassiosira sinica* YG–2017 isolate MC1477	0.03	0.03	0.03	0.03	0.03	0.03	0.03	0.01	0.01	0.01	0.02	0.02	0.01	0.02	0.02	0.01	0.01	0.00		
20. *Thalassiosira minicosmica* isolate MC544	0.03	0.03	0.03	0.03	0.03	0.03	0.03	0.01	0.01	0.01	0.02	0.02	0.01	0.03	0.02	0.01	0.02	0.01	0.01	0.00

Table 4. Pairwise uncorrected p–distances of 20 strains based on the partial LSU rDNA gene.

	1	**2**	**3**	**4**	**5**	**6**	**7**	**8**	**9**	**10**	**11**	**12**	**13**	**14**	**15**	**16**	**17**	**18**	**19**	**20**
1. *Conticribra sinica* strain LCH 2D3	0.00																			
2. *Conticribra sinica* strain LCH18	0.00																			
3. *Conticribra weissflogii* strain CCMP1010	0.08	0.08																		
4. *Conticribra weissflogii* strain RCC3389	0.08	0.08	0.03																	
5. *Conticribra guillardii* strain CC03–04	0.09	0.09	0.05	0.06																
6. *Conticribra guillardii* strain CCMP988	0.09	0.09	0.05	0.06	0.00															
7. *Conticribra weissflogiopsi*s isolate SMDC01212	0.07	0.07	0.03	0.04	0.05	0.05														
8. *Thalassiosira minuscula* strain CCMP1093	0.08	0.08	0.08	0.08	0.09	0.09	0.08													
9. *Thalassiosira gravida* voucher CCMP986	0.09	0.09	0.09	0.09	0.09	0.09	0.09	0.03												
10. *Thalassiosira punctigera* strain FB02–06	0.09	0.09	0.08	0.08	0.09	0.09	0.09	0.03	0.03											
11. *Thalassiosira nordenskioeldii* strain FB02–19	0.09	0.09	0.07	0.08	0.09	0.09	0.09	0.06	0.07	0.07										
12. *Thalassiosira profunda* isolate CNS00050	0.12	0.12	0.13	0.12	0.13	0.13	0.12	0.08	0.10	0.09	0.08									
13. *Thalassiosira curviseriata* strain RCC5154	0.09	0.09	0.09	0.09	0.09	0.09	0.09	0.05	0.06	0.06	0.03	0.08								
14. *Thalassiosira nodulolineata* strain BEN02–33	0.12	0.12	0.12	0.11	0.12	0.12	0.11	0.09	0.09	0.09	0.09	0.08	0.09							
15. *Thalassiosira secreta* Yli–2019a isolate MC1494	0.14	0.14	0.13	0.13	0.15	0.15	0.13	0.12	0.13	0.13	0.11	0.10	0.12	0.05						
16. *Thalassiosira minima* strain CCMP990	0.09	0.09	0.07	0.08	0.09	0.09	0.08	0.05	0.06	0.06	0.02	0.08	0.02	0.08	0.11					
17. *Thalassiosira hispida* strain RCC2521	0.08	0.08	0.07	0.08	0.08	0.08	0.08	0.04	0.05	0.04	0.04	0.09	0.04	0.09	0.12	0.04				
18. *Thalassiosira diporocyclus* isolate MC1466	0.10	0.10	0.09	0.09	0.09	0.09	0.10	0.04	0.04	0.04	0.07	0.10	0.07	0.09	0.14	0.07	0.05			
19. *Thalassiosira sinica* YG–2017 isolate MC1477	0.09	0.09	0.08	0.07	0.08	0.08	0.08	0.03	0.03	0.02	0.07	0.10	0.06	0.09	0.13	0.05	0.04	0.02		
20. *Thalassiosira minicosmica* isolate MC544	0.09	0.09	0.08	0.09	0.09	0.09	0.09	0.02	0.03	0.03	0.06	0.09	0.06	0.10	0.13	0.06	0.04	0.04	0.03	0.00

Table 5. Comparison of morphological characteristics of *Conticribra sinica* sp. nov. and other species in *Conticribra*.

Species/Feature		***C. sinica***	***C. tricircularis***	***C. nevadica***	***C.guillardii***	***C.weissflogii***	***C. weissflogiopsis***
Diameter (μm)		13–21.7	22–29	11–20	4–14	5–32	7.4–21.6
Cribra		Continuous	(Semi) continuous	Semi–continuous	Continuous	Continuous	Continuous
Marginal fultoportulae (mf)	Number of rings	1	3	1	1	1	1
	Position	On junction of valve face and mantle	On margin	On junction of valve face and mantle	On junction of valve face and mantle	On mantle	On mantle
	Density in 10 μm	11–15	—	8–10	7–8	9–16	10–12
	External opening	Tube	Tube, spinelike	Tube	Tube	Tube	Tube
	Number of satellite pores	4	4	2(4?)	4	4	4
Valve face fultoportulae	Number	4–12	Absent	Absent	0–3	Many on subcenter	2–12
	Number of satellite pores	3–4	—	—	2–4	3–5	3–4
Rimoportula	Number	1	1	1	1	1	1
	Location	Replace mf	Replace mf	Replace mf	Replace mf	Replace mf	Replace mf
Cingulum	Valvocopula	Fine pore, oblique rows	Fine pore, oblique rows	Fine pore, oblique rows	Fine pore, oblique rows	Fine pore, oblique rows	Fine pore, oblique rows
	Band opening	Irregular	—	—	Dextral	Sinistral	Dextral
References		Current study	Stachura–Suchoples & Williams (2009)	Stachura–Suchoples & Williams (2009)	Hasle et al. (1978)	Fryxell et al. (1981)	Park & Lee (2014)

Fottea, Olomouc, 22(2): 238–255, 2022
DOI: 10.5507/fot.2021.024

(Stachura–Suchoples & Williams 2009). The two fossil species *C. tricircularis* and *C. nevadica* were previously transferred to the genus *Spicaticribra* based on the the cribra pattern on the inner valve and the principle of preferential naming principles (Khursevich & Kociolek 2012). The two fossil species were compared with the genus *Spicaticribra*, revealing some significant differences. First, the rimoportula replaced marginal fultoportulae in the two fossil species, but rimoportula are located near the marginal fultoportulae in *Spicaticribra*. Second, the external tube of fultoportulae in the two fossil species had a long tubular extension, but the genus *Spicaticribra* does not exhibit an external tube and the fultoportulae opening is only slightly elevated from the valve. Third, the central areolae are usually larger (usually 3–6 times) than other valve face areolae on the external valve in the genus *Spicaticribra* compared to the two fossil species. Finally, external areolae were round and covered by long, spicate, anastomosing cribra internally in the genus *Spicaticribra*, while in the two fossil species, the areolae were loculate, open to the outside by circular foramina, and internally by (semi–)continuous cribra, consisting of linearly arranged pores (Johansen et al. 2008; Stachura–Suchoples & Williams 2009; Tuji et al. 2012; Gallo–Sánchez et al. 2015). On the basis of these observations, it is not appropriate to transfer the two fossil species to the genus *Spicaticribra*, but they should instead be classified as being within the genus *Conticribra*, as also suggested by Downey et al. (2021).

Acknowledgements
This research was funded and supported by National Natural Science Foundation of China (No. 31770222), and Biodiversity Survey and Assessment Project of the Ministry of Ecology and Environment, China (No. 2019HJ2096001006). We would like to thank Bingwei Xing, Xiaodie Jiang, and Bo Long for help in the field and in the preparation of samples for microscopy.

References

Alverson, A.J.; Jansen, R. & Theriot E.C. (2007): Bridging the Rubicon Phylogenetic analysis reveals repeated colonizations of marine and fresh waters by thalassiosiroid diatoms. – Molecular Phylogenetics and Evolution 45: 193–210.

Felsenstein, J. (1981): Evolutionary trees from DNA sequences: A maximum likelihood approach. – Journal of Molecular Evolution 17: 368.

Fryxell, G.A. & Hasle, G.R. (1977): The genus Thalassiosira: Some species with a modified ring of central strutted processes. – Beihft zur Nova Hedwigia 54: 67–89.

Gallo–Sánchez, L.J.; Sala, S.E.; Guerrero–Tizzano, J.M. & Flórez–M M.T. (2017): First report of the genus spicaticribra Johansen, Kociolek and Lowe in a Colombian reservoir and revision of the infrageneric taxa present in South America. – Bulletin of Faculty of Education Nagasaki University Educational Science 37: 43–49.

Guindon, S. & Gascuel, O. (2003): A simple, fast, and accurate algorithm to estimate large phylogenies by maximum likelihood. – Systematic Biology 52: 696.

Hall, T.A. (1999): BioEdit: a user–friendly biological sequence alignment editor and analysis program for Windows 95/98/NT. – Nucleic Acids Symposium Series 41 : 95–98.

Hasle, G.R. (1978): Some freshwater and brackish water species of the diatom genus Thalassiosira Cleve. – Phycologia 17: 263–292.

Johansen, J.; Kociolek, P. & Lowe, R. (2008): Spicaticribra kingstonii, gen. nov. et sp. nov. (Thalassiosirales, Bacillariophyta) from Great Smoky Mountains National Park, U.S.A. – Diatom Research 23: 367–375.

Kaczmarska, I.; Beaton, M.; Benoit, A.C. & Benoit, L.K. (2005): Molecular phylogeny of selected members of the order Thalassiosirales (Bacillariophyta) and evolution of the fultoportula. – Journal of Phycology 42: 121–138.

Downey, K.M.; Julius, M.L.; Theriot, E.C. & Alverson, A.J. (2021): Phylogenetic analysis places Spicaticribra within Cyclotella. – Diatom Research 36: 93–99.

Khursevich, G. & Kociolek, J.P. (2012): A preliminary, worldwide inventory of the extinct, freshwater fossil diatoms from the orders Thalassiosirales, Stephanodiscales, Paraliales, Aulacoseirales, Melosirales, Coscinodiscales, and Biddulphiales. – Nova Hedwigia Beiheft 141: 315–364.

Li, Y.; Gao, Y.Q. & Gao, X.H. (2018): Morphology and molecularphylogeny of Thalassiosira sinica sp. nov. (Bacillariophyta) with delicate areolae and fultoportulae pattern. – European Journal of Phycology 53: 122–134.

Li, Y.; Guo, Y.Q. & Lundholm, N. (2020): Description of Thalassiosira secreta sp. nov. (Bacillariophyta), unique with fultoportulae hidden inside the central areola. – European Journal of Phycology 55: 39–48.

Medlin, L.K & Kaczmarska, I. (2004): Evolution of the diatoms: V. Morphological and cytological support for the major clades and a taxonomic revision. – Phycologia 43: 245–270.

Parr, J.F.; Taffs, K.H. & Lane, C. M. (2004): A microwave digestion technique for the extraction of fossil diatoms from coastal lake and swamp sediments. – Journal of Paleolimnology 31: 383–390.

Park, J.S. & Lee, J.H. (2014): Description of the pseudocryptic species Conticribra weissflogiopsis sp. nov. (Thalassiosirales, Bacillariophyta) isolated from brackish waters in Korea, based on its cingulum structure and molecular analysis. – Phytotaxa 191: 115–128.

Posada, D. (2006): Modeltest Server: a web–based tool for the statistical selection of models of nucleotide substitution online. – Nucleic Acids Research 34:700–703.

Qi, Y.Z. (1995): Flora algarum sinicarum aquae dulcls, tomus IV, Bacillariophyta, Centricae. – 114 pp., Science Press, Beijing.

Ronquist, F. & Huelsenbeck, J.P. (2003): MrBayes 3: Bayesian phylogenetic inference under mixed models. – Bioinformatics 19: 1572–1574.

Round, F.E.; Crawford, R.M. & Mann, D.G. (1990): The Diatoms. Biology and morphology of the genera. – 747 pp., Cambridge University Press, Cambridge.

Stachura–Suchoples, K. & Kulikovskiy, M. (2014): Freshwater tolerance of Conticribra weissflogii in continental waters. – Nova Hedwigia 143: 485–495.

Stachura–Suchoples, K. & Williams, D.M. (2009): Description of Conticribra tricircularis, a new genus and species of Thalassiosirales, with a discussion on its relationship to other continuous cribra species of Thalassiosira Cleve (Bacillariophyta) and its freshwater origin. – European Journal of Phycology 44: 477–486.

Thompson, J.D.; Gibson, T.J.; Plewniak, F.; Jeanmougin, F. & Higgins, D.G. (1997): The CLUSTAL_X Windows Interface: Flexible Strategies for Multiple Sequence Alignment Aided by Quality Analysis Tools. – Nucleic Acids Research 25: 4876–4882.

Tuji, A.; Leelahakriengkrai, P. & Peerapornpisal, Y. (2012): Distribution and phylogeny of Spicaticribra kingstonii–rudis species complex. – Memoirs of National Museum Natural Science of Tokyo 48: 139–148.

Yu, P.; Kociolek, J.P.; You, Q.M. & Wang, Q.X. (2019): Three new freshwater species of the genus Achnanthidium (Bacillariophyta, Achnanthidiaceae) from Taiping Lake, China. – Fottea 19: 33–49.

Supplementary material

The following supplementary material is available for this article:

Table S1. Specimen information and list of sequences downloaded from the GenBank database.

Supplementary references

This material is available as part of the online article (http://fottea.czechphycology.cz/contents)

Received July 21, 2021
Accepted November 2, 2021